Dalton Transactions

Accepted Manuscript

This article can be cited before page numbers have been issued, to do this please use: B. Bertrand, A. S. Romanov, M. Brooks, C. Schmidt, I. Ott, M. A. O'Connell and M. Bochmann, *Dalton Trans.*, 2017, DOI: 10.1039/C7DT03189K.

This is an Accepted Manuscript, which has been through the Royal Society of Chemistry peer review process and has been accepted for publication.

Accepted Manuscripts are published online shortly after acceptance, before technical editing, formatting and proof reading. Using this free service, authors can make their results available to the community, in citable form, before we publish the edited article. We will replace this Accepted Manuscript with the edited and formatted Advance Article as soon as it is available.

You can find more information about Accepted Manuscripts in the author guidelines.

Please note that technical editing may introduce minor changes to the text and/or graphics, which may alter content. The journal's standard Terms & Conditions and the ethical guidelines, outlined in our author and reviewer resource centre, still apply. In no event shall the Royal Society of Chemistry be held responsible for any errors or omissions in this Accepted Manuscript or any consequences arising from the use of any information it contains.

ROYAL SOCIETY OF CHEMISTRY

rsc.li/dalton

View Article Online
DOI: 10.1039/C7DT03189K

Synthesis, Structure and Cytotoxicity of Cyclic (Alkyl)(Amino) Carbene and Acyclic Carbene Complexes of Group 11 metals

Benoît Bertrand,[a]* Alexander S. Romanov,[a] Mark Brooks,[b] Claudia Schmidt,[c] Ingo Ott,[c] Maria O'Connell,[b]* and Manfred Bochmann[a]*

[a] School of Chemistry, University of East Anglia, Norwich NR4 7TJ, UK

[b] School of Pharmacy, University of East Anglia, Norwich NR4 7TJ, UK

[c] Institute of Medicinal and Pharmaceutical Chemistry, Technische Universität Braunschweig, Beethovenstrasse 55, D-38106 Braunschweig, Germany

Abstract

A series of complexes of cyclic (alkyl)(amino)carbene (CAAC) complexes of copper, silver and gold have been investigated for their antiproliferative properties. A second series of acyclic carbene (ACC) complexes of gold(I) were prepared by nucleophilic attack on isocyanide complexes by amines and amino esters, to give (ACC)AuCl, $[(ACC)Au(PTA)]^+$ (PTA = triazaphosphaadamantane), as well as mixed-carbene compounds $[(CAAC)Au(ACC)]^+$. Representative complexes were characterised by X-ray diffraction which confirmed the mononuclear linear structures without close intermolecular contacts or aurophilic interactions. The redox properties of these complexes have been determined. The compounds were tested against a panel of human cancer cell lines including leukemia (HL 60), breast adenocarcinoma cells (MCF-7) and human lung adenocarcinoma epithelial cell lines (A549), which show varying degrees of cisplatin resistance. The pro-ligand iminium salts and the PTA complexes were non-toxic. By contrast, the CAAC complexes show high cytotoxicity, with IC_{50} values in the sub-micromolar to ~100 nanomolar range, even against cisplatin-insensitive MCF-7 and A549 cells. Cationic bis-carbene complexes $[(^{Me2}CAAC)_2M]^+$ (**6** – **8**, M = Cu, Ag and Au) proved particularly effective. The mechanism of cell growth control by these complexes remains to be established, although possible modes of action such as inhibition of thioredoxin reductase (TrxR), which is a common pathway for gold NHC compounds, or the formation of reactive oxygen species (ROS) through redox processes, could be ruled out as primary pathways.

Introduction

Carbene complexes of copper(I), silver(I) and gold(I) have been shown to display promising activities as antiproliferative agents towards a large number of cancer cell lines. Gold

View Article Online
DOI: 10.1039/C7DT03189K

complexes have been extensively studied, and their structures and cytotoxicity profiles have been the subject of a number of reviews.[1-6] Copper is an essential trace element and participates in a wide variety of catalytic functions in the body. Its homeostasis is guaranteed by different active transporters and chaperones. Copper complexes are being discussed in connection with developing treatments against a range of diseases, including neurodegenerative diseases, Alzheimer's and Parkinson's disease, as well as cancers.[7] Most of the compounds studied for anti-cancer activity are based on copper(II), and its cytotoxic activity is thought to be possibly related to its redox behaviour and generation of reactive oxygen species (ROS), to mitochondrial toxicity, to binding to intracellular thiols and interference in respiratory processes, as well as DNA cleavage and activation of apoptotic pathways in cancer cells.[8-11]

Carbene complexes of silver-too, have become attractive for their cytotoxic activity, which in some cases exceeds that of gold analogues.[12-16] The ligands used in these compounds are *N*-heterocyclic carbenes (NHCs) based on the imidazole framework and may be mono- or bi-dentate. NHC complexes generally fall into two categories: (i) mono-carbene adducts of metals salts that also carry a labile ligand X, such as in (NHC)MX, usually X = halide, where the X ligand can be expected to be readily substituted under physiological conditions and is susceptible to substitution by intracellular thiols; (ii) ionic bis-carbene complexes $[M(NHC)_2]^+X^-$, which may be redox active but can only bind to thiols after carbene dissociation. In any case, silver NHC complexes are known for their lability and have long been used as NHC transfer reagents for the synthesis of NHC complexes of other metals.[17,18] This implies that the structural integrity of (NHC)Ag compounds under physiological conditions cannot be taken for granted, so that establishing quantitative structure-activity relationships may not be straightforward.

In the present study we have chosen cyclic (alkyl)(amino)carbene (CAAC) ligands[19-21] coordinated to coinage metals to investigate the potential of these complexes as anti-proliferative agents. CAAC ligands have the advantage over NHCs that they bind significantly more strongly and are not prone to dissociation.[22] For example, CAAC ligands have been found capable of forming stable complexes even with zero-valent gold and copper.[23] For these reasons CAAC silver complexes are rather poor carbene transfer agents; for example they failed to give the expected carbene transfer to rhodium and ruthenium targets.[24] These characteristics are however beneficial for biological applications, as further supported by recent results on polycyclic CAAC complexes reported by Waldmann and co-workers.[25]

View Article Online
DOI: 10.1039/C7DT03189K

We also report the extension of carbene anti-cancer complexes to acyclic carbenes, in combination with CAAC and other ligands. Acyclic carbenes (ACC) offer the advantage of facile modification and functionalization via a common precursor and provide a potentially very versatile method for improving solubility, cell uptake and selectivity of cytotoxicity. Although acyclic carbene adducts of gold were among the first examples of carbene complexes to be reported,[26] their biological activity has hardly been explored.[27]

Results and Discussion

Synthesis and Structure. The compounds (CAAC)MCl **1** – **5** (M = Cu, Ag, Au, Chart I) and of the bis-carbene compounds [(^{Me2}CAAC)$_2$M]X (**6**, M = Cu, X = I; **7**, M = Ag, X = OTf; **8**, M = Au, X = Cl) were prepared following previously reported procedures.[19c,21,22a,24] Due to steric hindrance bis-CAAC complexes can be obtained only for methyl- and ethyl substituted CAAC ligands but not for adamantyl-substituted CAAC. The iminium salt ligand precursors ^{Me}**LH**, ^{Et}**LH** and ^{Ad}**LH** were also included in the toxicity testing programme for comparison. All the metal complexes are mononuclear in solution and in the solid state.

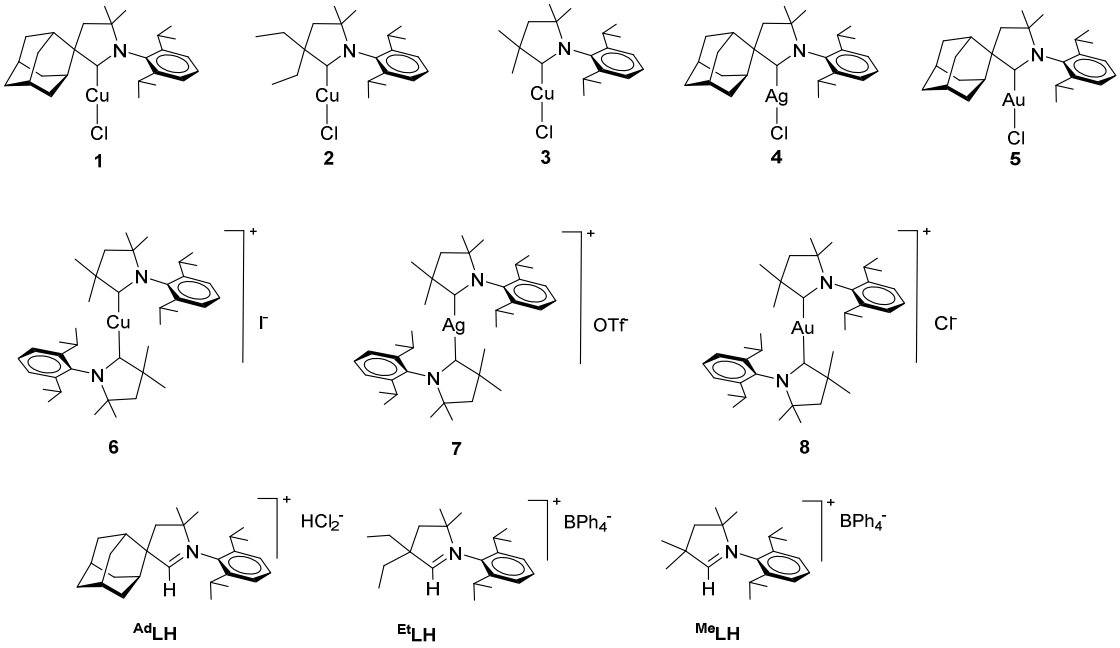

Chart I: Structure of the CAAC-M(I) complexes **1**-**8** and the corresponding pro-ligands.

Complexes with a combination of CAAC and acyclic carbene ligands were obtained by nucleophilic addition of amines and amino esters to gold(I) isocyanide complexes,[26] as

View Article Online
DOI: 10.1039/C7DT03189K

outlined in Scheme 1. Both neutral complexes (ACC)AuCl and ionic complexes $[(L)Au(ACC)]^{+}X^{-}$ were prepared to evaluate the influence of charge and solubility (ACC = acyclic carbene; L = ^{Ad}CAAC or triazaphosphaadamantane, PTA). The reaction of gold isocyanide complexes (RNC)AuCl (R = xylyl, ^{t}Bu) with pyrrolidine in dichloromethane at room temperature in the dark gave compounds **9a** and **9b** as white powders. Similarly, the reaction of sarcosine hydrochloride in acetonitrile in the presence of potassium carbonate afforded the amino acid derivatives **10a** and **10b** as orange to purple powders in good yields. The chloride ligands in **9** and **10** can be readily be substituted by PTA, chosen because of its water solubility, to give the ionic complexes **11a,b** and **12a,b**, respectively (Scheme 1). The structures of **11a** and **11b** were confirmed by X-ray crystallography (*vide infra*). In solution **12a** appears as a mixture of the two possible orientations of the sarcosine substituent of the ACC ligand in a ratio of approximately 0.75:0.25, while complex **12b** exists in solution as a mixture of all four possible stereoisomers of the ACC ligand; these lead to distinct ^{1}H NMR resonances for the N-H hydrogen with an integration ratio of approximately 0.1:0.2:0.2:0.5.

The reaction of (^{Ad}CAAC)AuCl with xylyl isocyanide and silver hexafluoroantimonate in dichloromethane under anhydrous conditions afforded the isocyanide complex **13a**, which reacted with pyrrollidine in acetonitrile gave the mixed-carbene complex **14a** as a white powder in 76% yield.

View Article Online
DOI: 10.1039/C7DT03189K

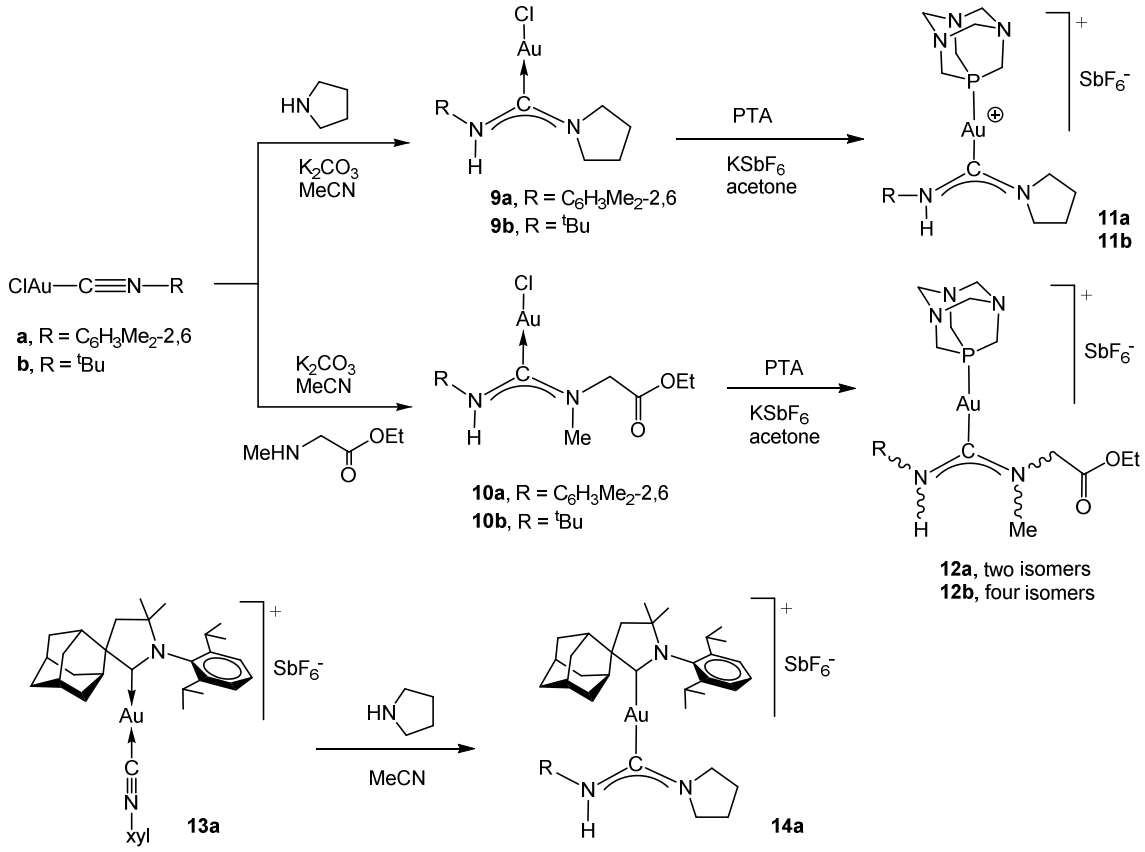

Scheme 1. Synthesis of neutral and ionic gold(I) complexes of acyclic carbenes

X-ray diffraction studies. The molecular structures of representative neutral and ionic ACC complexes with and without amino acid substituents were determined by X-ray diffraction (Figure 1). The structures of the CAAC complexes **13a** and **14a** are shown in Figure 2. All compounds show an almost linear coordination geometry, with the largest deviation observed for the bulky mixed-carbene complex **14a** (C1–Au–C28 173.4(1)°). The Au–C (*ca.* 2.00 Å) and Au–Cl (*ca.* 2.29 Å) bond lengths deviate within the error of the experiment for the complexes **9a**, **10a** and **10b** while being almost equidistant with other (ACC)AuCl reported in the literature.[28] The Au–C bond length for complex **11a** is elongated by 0.06 Å compared to complexes **9**–**10** due to moderate structural *trans*-influence of the phosphine (PTA) ligand *vs.* chloride anion, in accordance with the general trend.[29] The mixed-carbene complex **14a** shows that the Au–C_{CAAC} bond length is slightly shorter than Au–C_{ACC}. The open chain carbene ligands possess an essentially planar geometry with N–C–N angles greater than 116°, similar to the values previously observed for acyclic carbene ligands.[28] None of complexes show aurophilic metal-metal interactions. The molecules are

View Article Online
DOI: 10.1039/C7DT03189K

arranged into a three-dimensional network of weak interactions, based on N1–H1A···X (X = N, O, or F) hydrogen bonds between neighbouring molecules.

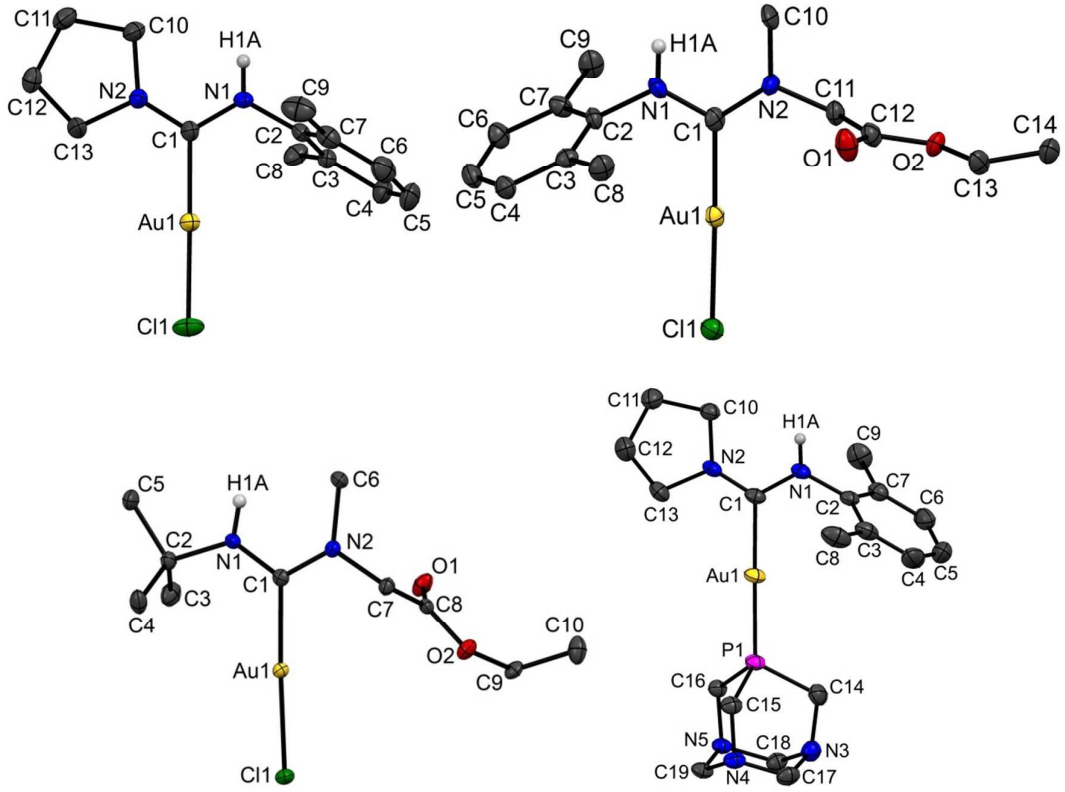

Figure 1. Molecular structures of **9a** (top left), **10a** (top right), **10b** (bottom left) and the cation in **11a** (bottom right). Ellipsoids are shown at the 50% level. Except for N-H, hydrogen atoms are omitted for clarity. Selected bond distances [Å] and angles [°]: **9a**: Au1–C1 1.999(3), Au1–Cl1 2.2891(8), C1–N1 1.342(4), C1–N2 1.323(4); C1–Au1–Cl1 178.68(9), N1–C1–N2 117.6(3). **10a**: Au1–C1 2.006(5), Au1–Cl1 2.2977(12), C1–N1 1.325(6), C1–N2 1.342(6); C1–Au1–Cl1 176.37(15), N1–C1–N2 117.3(4). **10b**: Au1–C1 2.011(2), Au1–Cl1 2.2929(5), C1–N1 1.324(2), C1–N2 1.340(2); C1–Au1–Cl1 176.78(5), N1–C1–N2 117.27(17). **11a**: Au1–C1 2.065(3), Au1–P1 2.2725(7), C1–N1 1.339(3), C1–N2 1.308(4); C1–Au1–P1 178.38(8), N1–C1–N2 118.6(2).

View Article Online
DOI: 10.1039/C7DT03189K

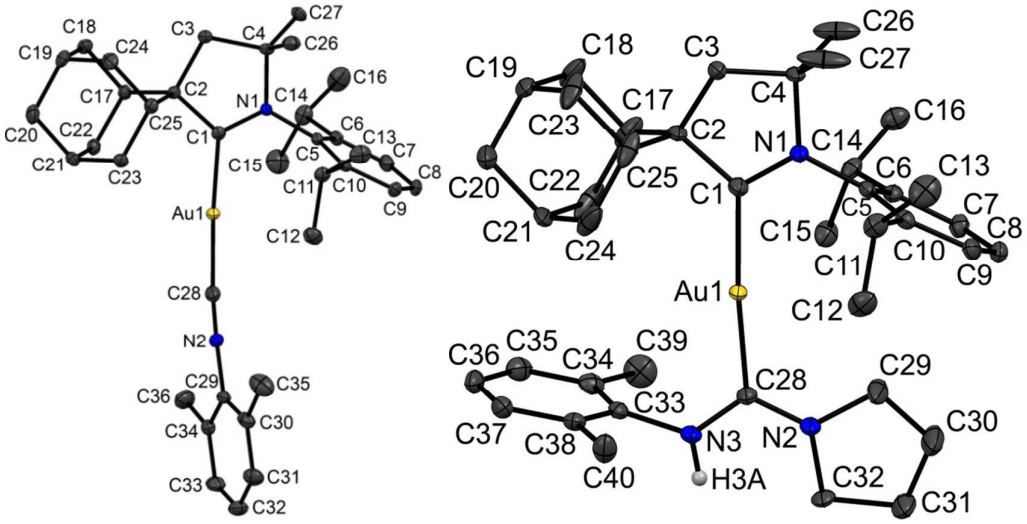

Figure 2. Molecular structures of the complex cations in **13a** (left), and **14a** (right). Ellipsoids are shown at the 50% level. Except for N-H, hydrogen atoms are omitted for clarity. Selected bond distances [Å] and angles [°]: **13a**: Au1–C1 2.034(3), Au1–C28 1.971(3), C1–C2 1.520(3), C1–N1 1.294(3), N2–C28 1.153(4); C1–Au–C28 174.51(11), Au–C28–N2 173.5(3). **14a**: Au1–C1 2.037(3), Au1–C28 2.043(3), C1–C2 1.530(4), C1–N1 1.302(4), N2–C28 1.326(4), C28–N3 1.337(4); C1–Au–C28 173.4(1), N2–C28–N3 116.4(3).

Electrochemistry. Cyclic voltammetry (CV) was used to analyse the redox behaviour of the CAAC copper, silver and gold complexes in MeCN and THF solutions using $[^{n}Bu_4N]PF_6$ or $[^{n}Bu_4N][B(C_6F_5)_4]$ as the supporting electrolytes (Table 1). The mono(carbene) silver chloride **4** in MeCN undergoes an irreversible reduction process with an anodic shift compared to the analogous copper (**1**, 240 mV) and gold compounds (**5**, 160 mV). A re-oxidation peak from the reduction process could not be detected at all scan rates from 0.05 to 2 Vs^{-1} in MeCN, likely due to reaction with the electrolyte or solvent. To solve this problem we have performed cyclic voltammetry in THF with the less nucleophilic supporting electrolyte $[^{n}Bu_4N][B(C_6F_5)_4]$. In this solvent the reduction process shows quasi-reversible character but at a significantly lower potential, with $E_{1/2}$ at -1.62 V (Figure 3). This indicates the feasibility of chemical reduction of the silver complex **4**. Its oxidation behaviour is very similar to the copper and gold analogues and at all scan rates shows one irreversible process without a back-peak, regardless of the solvent or supporting electrolyte.

View Article Online
DOI: 10.1039/C7DT03189K

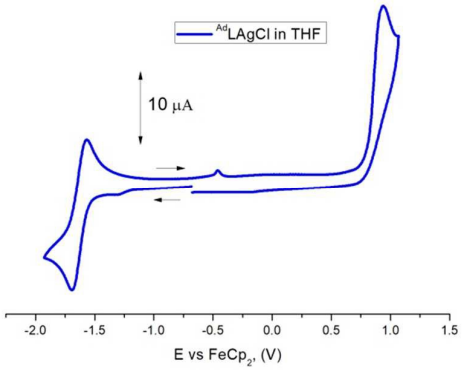

Figure 3. Full range cyclic voltammogram of (^{Ad}CAAC)AgCl (**4**), recorded using a glassy carbon electrode in THF solution (0.7 m*M*) with [^{n}Bu$_4$N][B(C$_6$F$_5$)$_4$] as supporting electrolyte (0.13 *M*).

The ionic homoleptic bis(carbene) complexes [(^{Me2}CAAC)$_2$M]X (M = Ag, X = OTf; M = Au, X = BF$_4$) show quasi-reversible one-electron reduction processes (Figure 4), with a significant anodic shift of the reduction potential $E_{1/2}$ by 200 mV compared to mono(carbene) metal chloride complexes (see Table 1). The quasi-reversibility of the reduction peak is witnessed by the negligible shift of 10 mV in the peak position E_p on increasing the scan rate and the peak-to-peak separation ΔE_p of 66–94 mV (at 100 mV/s), which is close to the ideal value of 59 mV for a one-electron reversible couple. Both silver (**7**) and gold (**8**) complexes show i_{pa}/i_{pc} values approaching unity, which is the ideal value for a reversible couple. For instance, the i_{pa}/i_{pc} ratio increases from 0.33 (at 50 mVs^{-1}) to 0.54 (at 2 Vs^{-1}) for silver [(^{Me2}CAAC)$_2$Ag]OTf and from 0.49 (at 50 mVs^{-1}) to 0.80 (at 2 Vs^{-1}) for gold complex [(^{Me2}CAAC)$_2$Au]BF$_4$ (Figure 4). The reversibility of the reduction process for silver (**7**) and gold (**8**) complexes is markedly different from the copper analogue [(^{Me2}CAAC)$_2$Cu]I (**6**), which shows quasi-reversible reduction only at high scan rates (0.5 to 2 Vs^{-1}). By contrast, at all scan rates the heteroleptic bis-carbene gold complex **14a** showed irreversible reduction (Figure 4), which was shifted cathodically by 220 mV compared to the homoleptic gold complex **8**.

Unlike the bis-carbene copper complex **6**, the irreversible oxidation of silver (**7**) and gold complexes **8** and **14a** is observed at high anodic potential as expected (1.33 V for silver and over 1.63 V for gold complexes) (Table 1). The oxidation potential for **8** was completely masked by solvent discharge (THF or MeCN), while silver (**7**) and the heteroleptic gold complex **14a** showed only partial overlap (Figure 4). We have previously reported that

View Article Online
DOI: 10.1039/C7DT03189K

chemical oxidation of mono-carbene and bis-carbene gold complexes with $PhICl_2$ produced photochemically unstable Au(III) complexes or decomposition products.[21]

Table 1. Formal electrode potentials (peak position E_p for irreversible and $E_{1/2}$ for quasi-reversible processes (*), *V*, *vs*. $FeCp_2$), onset potentials (*E, V*, *vs*. $FeCp_2$), peak-to-peak separation in parentheses for quasi-reversible processes (ΔE_p in mV), E_{HOMO}/E_{LUMO} (*e*V) and band gap values (ΔE, *e*V) for the redox changes exhibited by copper, silver, and gold complexes.

Complex	Reduction		E_{LUMO} eV	Oxidation			E_{HOMO} eV	ΔE eV
	$E_{M(I)/M(0)}$	$E_{onset\ red}$		E_{1st}	$E_{onset\ ox}$	E_{2nd}		
1 (^{Ad}L)CuCl [a]	–2.65	–2.60	–2.79	+0.67	+0.59	–	–5.98	3.19
2 (^{Et2}L)CuCl [a]	–2.82	–2.71	–2.68	+0.57	+0.35	+0.80	–5.74	3.21
3 (^{Me2}L)CuCl [a]	–2.70	–2.57	–2.82	+0.53	+0.24	+0.78	–5.63	2.81
4 (^{Ad}L)AgCl [a]	–2.41	–2.33	–3.06	+1.26	+1.06	–	–6.45	3.39
4 (^{Ad}L)AgCl [b]	–1.62*(125)	–1.55	–3.84	+0.93	+0.80	–	–6.19	2.35
5 (^{Ad}L)AuCl [a]	–2.57	–2.52	–2.87	+1.46	+1.34	–	–6.73	3.86
6 [(^{Me2}L)$_2$Cu]I [a]	–2.47*(65)	–2.39	–3.00	+0.02	–0.11	+0.27	–5.28	2.28
7 [(^{Me2}L)$_2$Ag]OTf [a]	–2.44* (66)	–2.37	–3.02	–[c]	–[c]	–	–	–
7 [(^{Me2}L)$_2$Ag]OTf [b]	–2.50* (94)	–2.43	–2.96	+1.33[c]	+1.16	–	–6.55	3.59
8 [(^{Me2}L)$_2$Au]BF_4 [a]	–2.22* (85)	–2.16	–3.23	–[c]	–[c]	–	–	–
14a [(^{Ad}L)Au(ACC)]$^+$ SbF_6^- [d]	–2.44	–2.31	–3.08	+1.63	+1.45	–	–6.84	3.76

[a] Recorded using a glassy carbon electrode, concentration 1.4 m*M* in acetonitrile, supporting electrolyte [^{n}Bu$_4$N][PF_6] (0.13 *M*), measured at 0.1 V s^{-1}. [b] Recorded using a glassy carbon electrode, concentration 0.7 m*M* in THF, supporting electrolyte [^{n}Bu$_4$N][$B(C_6F_5)_4$] (0.13 *M*), measured at 0.1 V s^{-1}. [c] Overlaps with solvent discharge. [d] Recorded using a glassy carbon electrode, concentration 2.0 m*M* in MeCN, supporting electrolyte [^{n}Bu$_4$N][PF_6] (0.13 *M*), measured at 0.1 V s^{-1}.

View Article Online
DOI: 10.1039/C7DT03189K

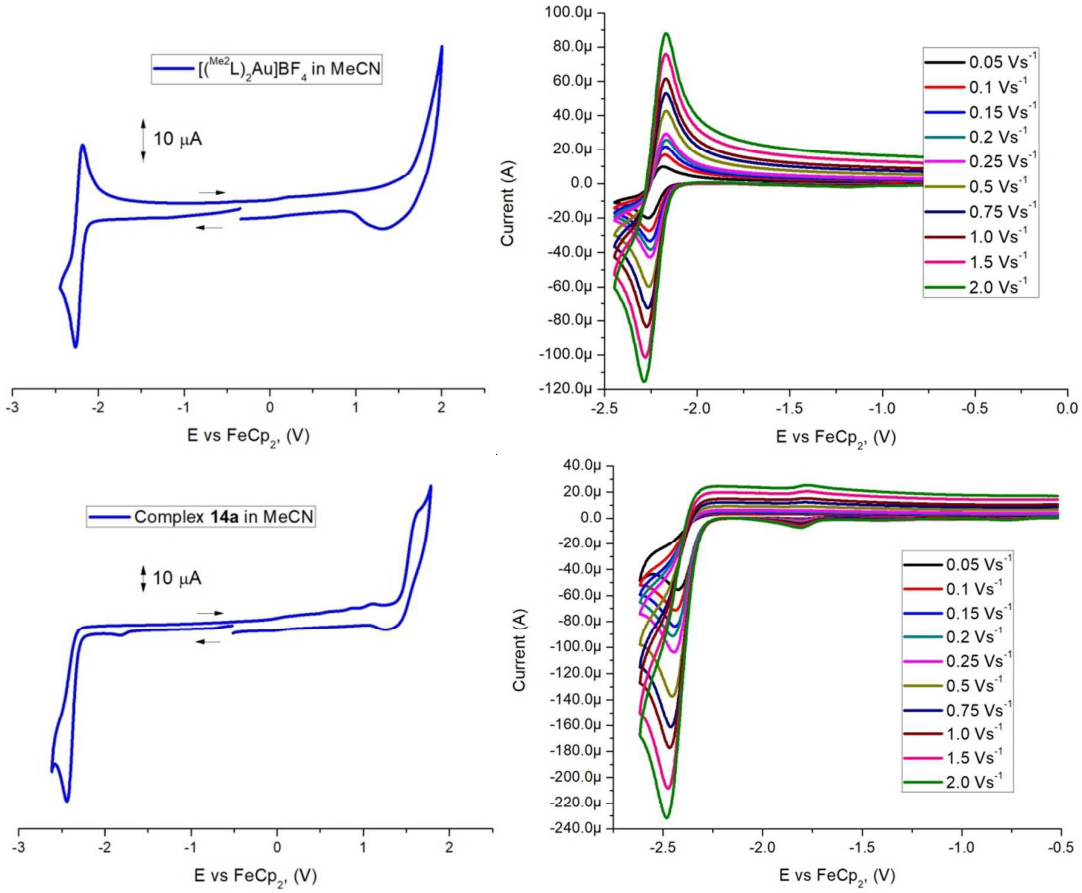

Figure 4. Top Left: full range cyclic voltammogram of homoleptic complex $[(^{Me2}CAAC)_2Au]BF_4$ (**8**). Top right: Varied scan rate behaviour recorded using a glassy carbon electrode in MeCN solution (1.4 m*M*) with $[^nBu_4N][PF_6]$ as supporting electrolyte (0.13 *M*). Bottom left: full range cyclic voltammogram of the open-chain carbene complex **14a**. Bottom right: Varied scan rate behaviour recorded using a glassy carbon electrode in MeCN solution (2.0 m*M*) with $[^nBu_4N][PF_6]$ as supporting electrolyte (0.13 *M*).

Antiproliferative properties on cancer cells in vitro. Although the complexes appeared to be poorly soluble in aqueous media, all compounds were soluble enough in DMSO not to precipitate when diluted with aqueous buffer solution up to 100 µM with 1% DMSO. Stock solutions of cisplatin were prepared in pure water. For an initial screening, the CAAC complexes **1** - **8** were selected for the determination of the IC_{50} on a panel of human cancer cell lines including leukemia (HL 60), breast adenocarcinoma cells (MCF-7) and human lung adenocarcinoma epithelial cells (A549) (Table 2).

Table 2. Effect of compounds **1-8**, **14a**, the pro-ligand iminium salts ^{Ad}**LH**, ^{Et}**LH** and ^{Me}**LH** and cisplatin on viability of cancer cell lines (IC_{50}, µM) after 72 h incubation.

View Article Online
DOI: 10.1039/C7DT03189K

Complex	HL 60	MCF-7	A549
1	0.14 ± 0.06	0.49 ± 0.02	17.4 ± 0.8
2	0.12 ± 0.01	0.32 ± 0.02	0.53 ±0.06
3	0.32 ± 0.04	0.57 ± 0.07	2.0 ± 0.5
4	0.18 ± 0.06	0.32 ± 0.10	5.7 ± 0.7
5	2.2 ± 0.2	4.1 ± 0.8	43.8 ± 0.4
6	0.13 ± 0.03	1.4 ± 0.6	0.31 ± 0.08
7	0.10 ± 0.01	1.2 ± 0.3	0.39 ± 0.06
8	0.09 ± 0.01	1.6 ± 0.6	0.5 ± 0.1
14a	0.10 ± 0.01	2.3 ± 0.9	6.1 ± 0.3
Cisplatin	3.7 ± 0.3	21.2 ± 3.9	33.7 ± 3.7
^{Ad}LH	8.0 ± 1.3	9.03 ± 0.09	> 50
^{Me}LH	> 50	> 50	> 50
^{Et}LH	> 50	19.5 ± 4.9	> 50

All three ligand precursors **^{R}LH** are non-toxic. The metal complexes, irrespective of whether they are neutral halides or of the ionic bis-carbene type, are particularly active on HL 60, and MCF-7 cell lines, with IC_{50} values from the low-micromolar to the ~100 nanomolar range. These complexes are substantially more active than cisplatin. The copper complexes **1** – **3** show high activity against HL-60 and MCF-7, with IC_{50} values in the low submicromolar range. Their activity against A549, a cell line which typically shows high cisplatin resistance, is about an order of magnitude lower. The exception here is the surprisingly low activity of (^{Ad}CAAC)CuCl **1** against A549, which contrasts with the low IC_{50} value of only 0.53 ±0.06 μM for the ethyl analogue, (^{Et}CAAC)CuCl **2**. The silver complex (^{Ad}CAAC)AgCl **4** is slightly more toxic than its copper analogue **1** on the MCF-7 cells. Overall **4** shows a similar trend: sub-micromolar activity against HL-60 and MCF-7 and low micromolar values against the more resistant A549 lines. These copper and silver CAAC complexes are an order of magnitude more potent than the gold complex **5**, which is less effective than copper and

View Article Online
DOI: 10.1039/C7DT03189K

silver against HL-60 and MCF-7 and, surprisingly, non-toxic against A549. In the series of adamantyl-substituted CAAC complexes, against HL-60, MCF-7 and A549 silver shows the highest and gold the lowest cytotoxicity: IC_{50}(**5**) > IC_{50}(**1**) ≥ IC_{50}(**4**). On the other hand, such a metal dependence has been not observed in the cationic series, for which very similar, and remarkably low, IC_{50} values were determined for all metals against each of the tested cancer cell lines. Indeed, all $[(CAAC)_2M]^+$ complexes **6** - **8** demonstrated very strong antiproliferative effects, with IC_{50} values down up to sub-micromolar levels, including against A549 cells which are particularly difficult to treat with cisplatin.

Varying the substituents on the CAAC ligand in the copper series leads to only small differences in activity against HL 60 and MCF-7 cell lines, while against A549 cells a dramatic substituent dependence of the cytotoxic properties was observed (IC_{50} = 17.4 ± 0.8; 0.53 ± 0.06 and 2.0 ± 0.5 μM for **1**, **2** and **3** respectively), indicating that ^{Et2}CAAC complexes are the most toxic of this series.

The acyclic carbene complexes **9** – **12** and **14a** were screened against lung (A549) and breast (MCF-7) cancer cells at concentrations of 10 and 100 μM. The cell viability was measured after 72 hours of incubation using the standard MTS assay (see experimental part). The results are reported in Figure 5.

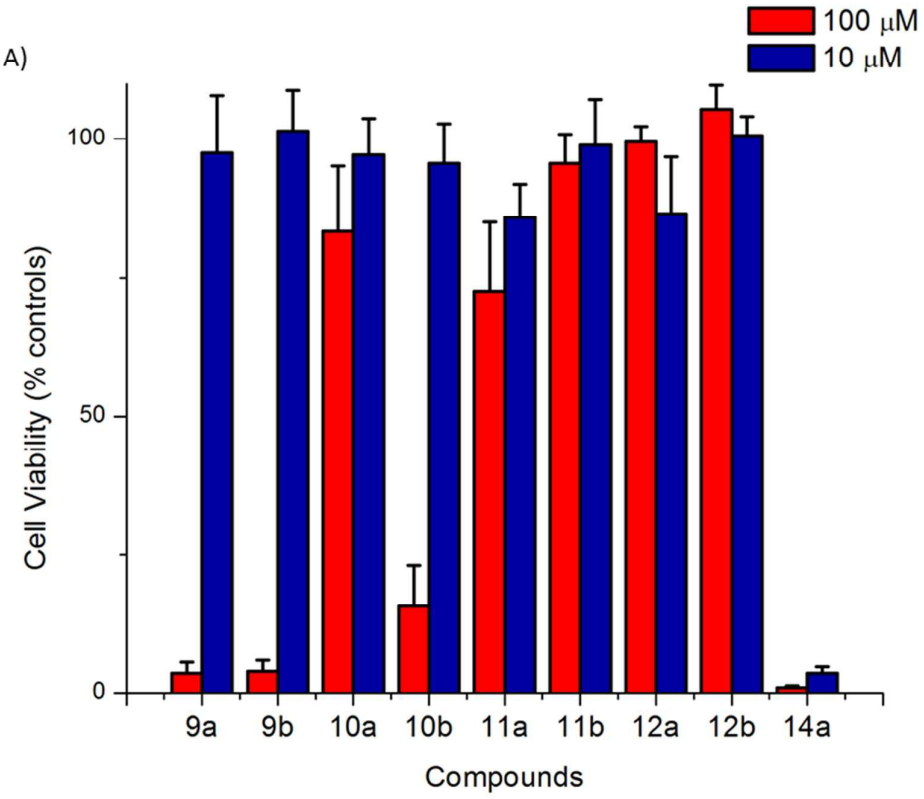

View Article Online
DOI: 10.1039/C7DT03189K

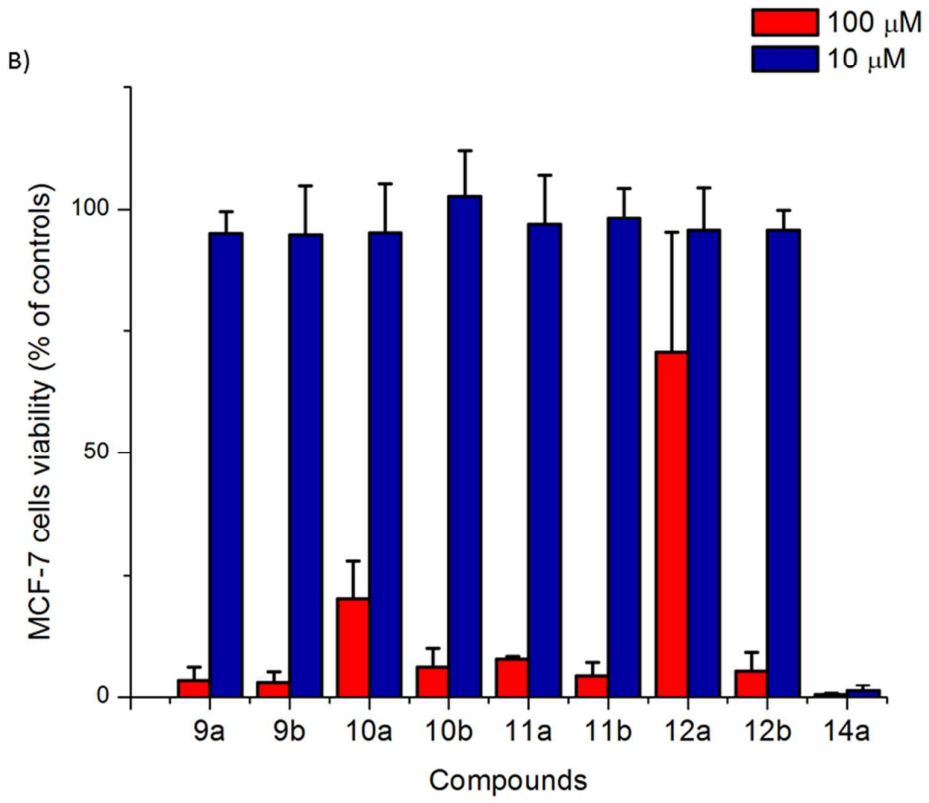

Figure 5: Inhibition of A) A549 cells and B) MCF-7 cells proliferation by ACC complexes **9 – 12** and **14a**; data represent the average ± standard error of three experiments.

None of the PTA complexes **11 - 12** showed any cell growth inhibition against the lung cancer cells at both tested concentrations (A549, Fig. 5A). In the chloro series **9 - 10**, compounds **9a**, **9b** and **10b** demonstrated a strong antiproliferative effect at 100 μM (cell viability of 4.2 ± 1.9, 3.8 ± 2.0 and 15.8 7.3 % respectively), while compound **10a** bearing an ACC ligand with 2,6-$Me_2C_6H_3$ and sarcosine substituents appeared completely inactive at both tested concentrations. None of the chloro and PTA complexes **9** – **12** showed any proliferative activity against MCF-7 at the lower concentration of 10 μM (Fig. 5B). Moreover, while complexes **9a**, **9b**, **10b**, **11a**, **11b** and **12b** completely inhibited cell growth at the higher concentration of 100 μM, the two complexes presenting the ACC ligand with the xylyl/sarcosine combination, **10a** and **12a**, appeared to have a reduced activity even at that high concentration (cell viability of 20.2 ± 7.7 and 71 ± 24 % for **10a** and **12a** respectively). Combined with the data against A549 cells, this suggests a deleterious effect of that particular substituent combination on the antiproliferative properties of these compounds.

View Article Online
DOI: 10.1039/C7DT03189K

By contrast, the mixed-carbene complex $[(^{Ad}CAAC)Au(ACC)]^+$ **14a** fully inhibited both A549 and MCF-7 cells growth at both high and low concentrations, making it the most promising complex of the ACC series. For that reason it is the only one that was used for the determination of IC_{50} against our human cancer cell lines panel (Table 2). Like all $[(CAAC)_2M]^+$ complexes, **14a** demonstrated IC_{50} values in the low to sub-micromolar range against the panel of tested cell lines (IC_{50} = 0.10 ± 0.01; 2.3 ± 0.9 and 6.1 ± 0.3 μM against HL60, MCF-7 and A549 cells respectively). This demonstrates the potential of using a mixed $[(CAAC)Au(ACC)]^+$ scaffold for the introduction of functionalities, for example as vectors to improve cell uptake selectivity or as imaging probes.

Mechanistic investigations: inhibition of TrxR Thioredoxin reductase (TrxR) is a homodimeric enzyme whose role consists of reducing thioredoxin in an NADPH-dependent manner. Thioredoxin (Trx) in turn reduces different proteins including peroxiredoxin (involved in the regulation of cellular level of hydrogen peroxide).[30] TrxR has been reported as a potential intracellular target for complexes of various metals, including Ru, Fe and Au.[31-33] Among those, Au(I)-NHC complexes were found to be particularly potent TrxR inhibitors.[3,4,34] Based on those finding we have tested our most toxic complexes **1**-**8** as potential TrxR inhibitors (see Experimental for details). We first performed a screening of all complexes at 10 μM against mammalian TrxR. The results are reported in Table 3.

Table 3. Effects of compounds **1 – 8** and **14a** and of the pro-ligand salts ^{Ad}**LH**, ^{Et}**LH** and ^{Me}**LH** on mammalian TrxR activity.

Complex	Inhibition at 10 μM (% control)[a]	IC_{50} ± SD (μM)[b]
1	17.6	n.d.
2	52.3	n.d.
3	43.0	n.d.
4	69.0	4.6 ± 0.3
5	91.6	2.6 ± 0.8
6	27.1	n.d.
7	56.8	6.8 ± 0.1

View Article Online
DOI: 10.1039/C7DT03189K

8	52.8	9.4 ± 1.3
^{Ad}**LH**	0.0	n.d.
^{Me}**LH**	0.0	n.d.
^{Et}**LH**	0.0	n.d.

[a] Results of only one experiment. [b] Data represent the average ± standard error of three experiments.

Although none of the copper containing compounds (**1 - 3** and **6**) showed any strong inhibitory effects on TrxR up to a concentration of 10 μM (less than 50% inhibition), we could notice a trend between the bulkiness of the CAAC ligand and the inhibitory activity of the corresponding Cu-Cl complexes. Indeed, the adamantyl complex **1** was much less potent than the ethyl and methyl complexes **2** and **3**. Moreover, for the same substituent (methyl) the coordinatively saturated bis-CAAC complex **6** was a much weaker TrxR inhibitor than its mono-CAAC analogue **3**. Those data are in good agreement with the reported mechanism of action of Au(I) complexes which involves the direct coordination of the metal centre to the selenocysteine residue of the active site of TrxR.[34] The silver and gold complexes, both in the mono- and bis-CAAC series, inhibited TrxR at the concentration of 10 μM. Those compounds where thus selected for the determination of their IC_{50} against mammalian TrxR. The IC_{50} values follow the trend (CAAC)MCl < $[(CAAC)_2M]^+$, as already noticed in the copper series. The best inhibitor was the mono-CAAC gold complex **5**. However the TrxR inhibition activity of **5** (IC_{50} = 2.6 ± 0.8 μM) is almost 10 times lower than that of reported NHC-Au-Cl complexes,[35] while **8** showed an inhibiting effect similar to the previously reported $[(NHC)_2Au]^+$ complexes.[36] In particular regarding gold complexes, the higher activity of monocarbene complexes versus biscarbene analogues has been observed in several recent studies.[36a,b,37] The decreased inhibitory activity of **5** compared to other monocarbene gold NHC complexes might be explained by the steric protection of the gold centre, which is expected to inhibit the ability of the gold centre to bind to the selenocyteine residue of the active site of TrxR.

Altogether, the data show that although inhibition of TrxR might account partially for the observed antiproliferative properties of some the CAAC compounds investigated here (complexes **4**, **5**, **7** and **8**), the IC_{50} values are an order of magnitude higher than the IC_{50}

View Article Online
DOI: 10.1039/C7DT03189K

values derived from cell growth inhibition. This leads to the conclusion that TrxR inhibition is most probably not the main mode of action of the CAAC class of compounds.

Mechanistic investigations: enhancement of ROS formation. Reactive oxygen species (ROS) are naturally produced by mitochondria and are involved in different intracellular processes. However, their production, location and quantity is tightly controlled. ROS overproduction can induce cellular stress leading to cell death.[38] We measured the intracellular ROS amount of A549 cells after incubation with the most toxic complexes **1** - **8** and **14a** for 24 hours (Figure 6).

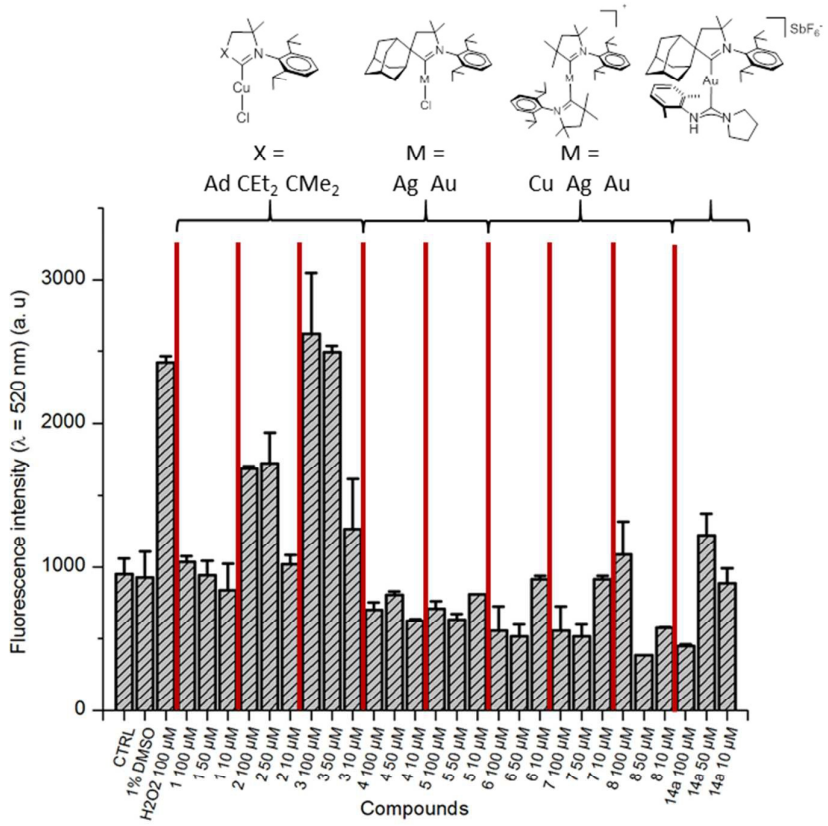

Figure 6: ROS measurement in A549 cells after 24 h incubation with complexes **1** - **8** and **14a**. Data represent the average ± standard error of three experiments.

In the CuCl series there is a clear correlation between the substituent on the CAAC ligand and the ability of the compounds to induce ROS production, with the least bulky ^{Me2}CAAC complex **3** inducing about the same amount of ROS production as the positive control H_2O_2, whereas the most bulky adamantly-substituted complex **1** presented the same amount of ROS as the negative control samples. The ^{Ad}CAAC complexes **1**, **4** and **5** did not trigger the formation of ROS. None of the cationic bis-CAAC complexes **6** - **8** led to ROS

View Article Online
DOI: 10.1039/C7DT03189K

formation either, despite the fact that they contain the sterically least demanding ^{Me2}CAAC ligand, and despite the differences in their oxidation potentials. Of course, these bis-carbene complexes lack readily available coordination sites, and overall the results suggest that the accessibility of the metal for further complexation is of particular importance for the generation of ROS. Moreover, while (NHC)AuCl and $[(NHC)_2Au]^+$ complexes have been reported to enhance the formation of intracellular ROS,[35,36a] we found that neither neutral (CAAC)AuCl **5** nor the homo- and heteroleptic bis-carbene cations $[(CAAC)_2Au]^+$ **8** and [(CAAC)Au(ACC)] **14a** are able to trigger an increase in intracellular ROS. These data, taken together with the relatively low inhibitory effect on TrxR, suggest that the mode of action of the CAAC-based complexes is different from that of their analogues with more labile NHC ligands. Evidently, the primary inhibitory mechanism of the new CAAC complexes remains to be established.

Conclusion

Acyclic carbene complexes of gold(I) are readily accessible from the reaction of the corresponding isocyanide complexes with amines, including amino acid esters. This method was explored for its potential for attaching bio-relevant substituents to non-labile carbene ligands. These ACC complexes, together with eight neutral and cationic CAAC-based complexes of Cu, Ag and Au, were screened for their antiproliferative properties on a panel of human cancer cells. Compared to the more conventional imidazolylidene-type NHC complexes, CAAC compounds offer the advantage that they are not prone to ligand exchange and retain their structural integrity in aqueous media and under physiological conditions. While none of the chloride or PTA derivatives demonstrated particularly promising cytotoxic effects, the CAAC-containing complexes showed interesting IC_{50} values down to sub-micromolar levels. In particular, the cationic $[(^{Me2}CAAC)_2M]^+$ complexes (**6** – **8**, M = Cu, Ag and Au) and the mixed-carbene complex $[(^{Ad}CAAC)Au(ACC)]^+$ **14a** proved to be the most potent of the series. The CAAC containing complexes appeared to only poorly inhibit TrxR, suggesting the TrxR inhibition by binding to the selenium site is unlikely to be the primary intracellular target. While Cu complexes with sterically less-hindered CAAC ligands appeared to enhance the formation ROS, none of the other CAAC-containing complexes seemed to do so up to a concentration of 100 μM. Overall, our study documents that CAAC-based complexes show promise for anticancer applications. The use of mixed CAAC/ACC combinations is of particular interest since it opens the way to further functionalization of this

View Article Online
DOI: 10.1039/C7DT03189K

scaffold. Studies to understand the possible mode of action of those compounds as well as their conjugation to bio-vectors are currently ongoing.

Experimental

General Remarks. Unless stated otherwise all reactions were carried out in air. Solvents were distilled and dried as required. The carbene ligands ^{Me2}CAAC, ^{Et2}CAAC, ^{Ad}CAAC,[19] and complexes [(^{Et2}CAAC)$_2$Cu]I,[22b] and (CAAC)MCl (M = Cu, Ag, Au; X = Cl, Br, I),[21-24] were obtained according to literature procedures. ^{1}H, ^{13}C{^{1}H} and ^{19}F NMR spectra were recorded using a Bruker Avance DPX-300 MHz NMR spectrometer. ^{1}H NMR spectra (300.13 MHz) and ^{13}C{^{1}H} (75.47 MHz) were referenced to CD_2Cl_2 at δ 5.32 (^{13}C, δ 53.84), C_6D_6 at δ 7.16 (^{13}C, δ 128.4), $CDCl_3$ at δ 7.26 (^{13}C, δ 77.16) or C_6D_5Br at δ 7.30 for the most downfield signal (^{13}C, δ 122.5) ppm. ^{19}F NMR spectra (282.4 MHz) were referenced externally to $CFCl_3$ and internally to C_6F_6 (δ_F -164.9). IR spectra were recorded using a Perkin-Elmer Spectrum One FT-IR spectrometer equipped with a diamond ATR attachment. Electrochemical experiments were performed using an Autolab PGSTAT 302N computer-controlled potentiostat. Cyclic voltammetry (CV) was performed using a three-electrode configuration consisting of either a glassy carbon macrodisk working electrode (GCE) (diameter of 3 mm; BASi, Indiana, USA) combined with a Pt wire counter electrode (99.99 %; GoodFellow, Cambridge, UK) and an Ag wire pseudoreference electrode (99.99 %; GoodFellow, Cambridge, UK). The GCE was polished between experiments using alumina slurry (0.3 μm), rinsed in distilled water and subjected to brief sonication to remove any adhering alumina microparticles. The metal electrodes were then dried in an oven at 100 °C to remove residual traces of water, the GCE was left to air dry and residual traces of water were removed under vacuum. The Ag wire pseudoreference electrodes were calibrated to the ferrocene/ferrocenium couple in MeCN at the end of each run to allow for any drift in potential, following IUPAC recommendations.[39] All electrochemical measurements were performed at ambient temperatures under an inert Ar atmosphere in MeCN containing complex under study (0.14 mM) and supporting electrolyte [^{n}Bu$_4$N][PF$_6$] (0.13 mM). Data were recorded with Autolab NOVA software (v. 1.11). Elemental analyses were performed by London Metropolitan University. Compound **9b** has been synthesized according to reported procedure.[28]

Synthesis of ClAu{C(NHxylyl)(pyrrolidine)} (**9a**)

View Article Online
DOI: 10.1039/C7DT03189K

Xylylisocyanide gold chloride (50 mg, 0.18 mmol, 1 eq.) was dissolved in dichloromethane. Pyrrolidine (49 mg, 0.90 mmol, 5 eq.) was added to this solution. The mixture was left overnight at room temperature in the dark, filtered through celite and then washed with saturated aqueous ammonium chloride solution. The clear solution was dried with sodium sulphate for 1h, filtered and the volatiles were removed under vacuum. The product was precipitated with a dichloromethane/hexane mixture to form a white powder which was dried under vacuum (47 mg, 0.14 mmol, 79%). Anal. Calcd for $C_{13}H_{18}N_2AuCl$ (434.7): C, 35.92; H, 4.17; N, 6.44. Found: C, 36.08; H, 4.25; N, 6.47. ^{1}H NMR ($CDCl_3$, 300 MHz): δ 7.13 (m, 3H, $H_{arom.\ xylyl}$), 6.61 (s, 1H, NH), 4.05 (t, $^3J_{H\text{-}H}$ = 9 Hz, 2H, H^1 or H^4), 3.40 (t, $^3J_{H\text{-}H}$ = 6 Hz, 2H, H^1 or H^4), 2.23 (m, 8H, Me_{xylyl} + H^2 or H^3), 2.00 (p, $^3J_{H\text{-}H}$ = 6 Hz, 2H, H^2 or H^3). $^{13}C\{^1H\}$ NMR ($CDCl^3$, 75 MHz): 190.9 (s, $C_{carbene}$), 137.5 (s, $C_{arom.\ ipso}$), 136.3 (s, $C_{arom.\ ortho}$), 128.8 (s, $CH_{arom.}$), 128.6 (s, $CH_{arom.}$), 56.1 (s, $CH_2^{1/4}$), 45.5 (s, $CH_2^{1/4}$), 25.6 (s, $CH_2^{2/3}$), 24.4 (s, $CH_2^{2/3}$), 19.2 (s, CH_3). IR ν_{max} (neat)/cm^{-1}: 3725 (NH), 1551 (carbene).

Synthesis of ClAuC(NHxylyl)(sarcosine) (10a)

Sarcosine hydrochloride (210 mg, 1.50 mmol) was dissolved in acetonitrile and stirred with potassium carbonate (207 mg, 1.5 mmol) for 1h. The resulting mixture was paper-filtered and (xylylNC)AuCl (110 mg, 0.30 mmol) was added and left to mix for an hour. The solution was purified by filtration through Celite, washing with ammonium chloride and drying over anhydrous Na_2SO_4 for 1h. This mixture was then paper-filtered and the volatiles were removed under vacuum. The product was precipitated with hexane and diethyl ether to give an orange powder (95 mg, 0.09 mmol, 66%). Anal. Calcd for $C_{14}H_{20}N_2O_2AuCl$ (480.74): C, 34.98; H, 4.19; N, 5.83. Found C, 35.02; H, 4.28; N, 5.91**.** ^{1}H NMR ($CDCl_3$, 300 MHz): δ 7.15 (m, 4H, $H_{arom.\ xylyl}$ + NH), 4.81 (s, 2H, NCH_2), 4.24 (q, $^3J_{H\text{-}H}$ = 7.0 Hz, 2H, OCH_3), 3.16 (s, 3H, NCH_4), 2.24 (s, 6H, $CH_{3\ xylyl}$), 1.31 (t, $^3J_{H\text{-}H}$ = 7 Hz, 3H, $CH_2\underline{CH_3}$). $^{13}C\{^1H\}$ NMR ($CDCl_3$, 75 MHz): 196.4 (s, $C_{carbene}$), 168.6 (s, C=O), 136.9 (s, $C_{arom.\ ipso}$), 136.3 (s, $C_{arom.\ ortho}$), 128.9 (s, $CH_{arom.}$), 128.8 (s, $CH_{arom.}$), 62.1 (s, OCH_2), 61.2 (s, NCH_2), 35.9 (s, NCH_3), 18.9 (s, $CH_{3\ xylyl}$), 14.3 (s, $CH_2\underline{CH_3}$). IR ν_{max} (neat)/cm^{-1}: 3219 (NH), 1745 (C=O), 1547 (carbene).

Synthesis of ClAuC(NH^{t}Bu)(Sarcosine) (10b)

The compound was prepared as described for 10a, from sarcosine hydrochloride (44 mg, 0.32 mmol) and *t*-butyl isocyanide gold chloride (50 mg, 16 mmol) in acetonitrile. Drying under vacuum resulting in a purple powder (58 mg, 0.27 mmol, 84%,). Anal. Calcd for $C_{10}H_{20}N_2O_2AuCl$ (432.7): C, 27.76; H, 4.66; N, 6.47. Found: C, 27.71; H, 4.70; N, 6.35. ^{1}H

View Article Online
DOI: 10.1039/C7DT03189K

NMR ($CDCl_3$, 300 MHz): δ 5.95 (s, 1H, NH), 4.85 (s, 2H, NCH_2), 4.22 (q, $^3J_{H-H}$ = 7 Hz, 2H, OCH_2), 2.96 (s, 3H, NCH_3), 1.65 (s, 9H, ^{t}Bu), 1.30 (t, $^3J_{H-H}$ = 7 Hz, 3H, $CH_2\underline{CH_3}$). $^{13}C\{^1H\}$ NMR ($CDCl_3$, 75 MHz): 193.6 (s, $C_{carbene}$), 168.9 (s, *C*=O), 62.7 (s, O*C*H_2), 62.0 (s, N*C*H_2), 55.1 (s, *C*$(CH_3)_3$), 34.6 (s, N*C*H_3), 31.8 (s, C(*C*$H_3)_3$), 14.27 (s, $CH_2\underline{CH_3}$). IR ν_{max} (neat)/cm^{-1}: 3364 (NH), 1734 (C=O), 1548 (carbene).

Synthesis of [(1,3,5-triaza-7-phosphaadamantane)Au{C(NHxylyl)(pyrrolidine)}]PF_6 (11a)

ClAu{C(NHxylyl)(pyrrolidine)} (42 mg, 0.10 mmol) was dissolved in acetone and 1,3,5-triaza-7-phosphaadamantane (PTA, 16 mg, 0.10 mmol) and potassium hexafluorophosphate (92 mg, 0.50 mmol) were added. The mixture was stirred overnight at room temperature, filtered and the acetone removed under vacuum. The product was taken up in dichloromethane and precipitated with hexane to give a white powder (60 mg, 0.07 mmol, 70%). ^{1}H NMR (DMSO, 300 MHz): δ 9.41 (s, 1H, NH), 7.21 (m, 3H, $H_{arom.}$), 4.45 (d, $^3J_{H-H}$ = 15 Hz, 3H, NCH_2N), 4.28 (d, $^3J_{H-H}$ = 15 Hz, 3H, NCH_2N), 4.02 (s, 6H, PCH_2N), 3.78 (t, $^3J_{H-H}$ = 6 Hz, 2H, H^1 or H^4), 3.40 (t, $^3J_{H-H}$ = 6 Hz, 2H, H^1 or H^4), 2.19 (s, 6H, $CH_{3\ xylyl}$), 2.05 (m, 2H, H^2 or H^3), 1.89 (m, 2H, H^2 or H^3). $^{13}C\{^1H\}$ NMR (DMSO, 75 MHz): ($C_{carbene}$ not visible), 138.2 (s, $C_{arom.\ ipso}$), 136.2 (s, $C_{arom.\ ortho}$), 128.2 (s, *C*$H_{arom.}$), 127.9 (s, *C*$H_{arom.}$), 71.7 (s, N*C*H_2N), 54.8 (s, *C*$H_2^{1/4}$), 47.0 (s, *C*$H_2^{1/4}$), 51.1 (broad s, P*C*H_2N), 30.8 (s, *C*$H_2^{2/3}$), 24.6 (s, *C*$H_2^{2/3}$), 18.6 (s, *C*$H_{3\ xylyl}$). $^{31}P\{^1H\}$ NMR (DMSO, 121 MHz): -51.2 (broad s, 1P, PTA), -144.2 (h, $^1J_{P-F}$ = 708 Hz, 1P, PF_6). IR ν_{max} (neat)/cm^{-1}: 3160 (NH), 1557 (carbene).

Synthesis of [(1,3,5-triaza-7-phosphaadamantane)Au{C(NH^{t}Bu)(pyrrolidine)}]PF_6 (11b)

The complex was prepared as described for **11a**, from ClAuC(NH^{t}Bu)(pyrrolidine) (27 mg, 0.07 mmol), 1,3,5-triaza-7-phosphaadamantane (11 mg, 0.07 mmol) and potassium hexafluorophosphate (64 mg, 0.35 mmol) as a white powder (35 mg, 0.05 mmol, 77%). Anal. Calcd for $C_{15}H_{30}N_5PAuPF_6$ (671.9): C, 28.60; H, 4.88; N, 10.42. Found: C, 28.62; H, 5.21; N, 10.20. ^{1}H NMR (DMSO, 300 MHz): δ 7.19 (s, 1H, NH), 4.57 (d, $^3J_{H-H}$ = 12 Hz, 3H, NCH_2N), 4.36 (d + s, $^3J_{H-H}$ = 12 Hz, 3H + 6H, NCH_2N + PCH_2N), 3.82 (broad s, 2H, *C*$H_2^{1/4}$), 3.28 (broad s, 2H, *C*$H_2^{1/4}$), 1.93 (broad s, 2H, *C*$H_2^{2/3}$), 1.81 (broad s, 2H, *C*$H_2^{2/3}$), 1.49 (s, 9H, ^{t}Bu). $^{13}C\{^1H\}$ NMR (DMSO, 75 MHz): 202.3 (s, $C_{carbene}$), 71.8 (d, $^3J_{P-C}$ = 8 Hz, N*C*H_2N), 55.9 (s, *C*$H_2^{1/4}$), 53.5 (s, *C*$(CH_3)_3$), 50.9 (broad s, P*C*H_2N), 46.1 (s, *C*$H_2^{1/4}$), 31.8 (s, C(*C*$H_3)_3$), 24.4 (s, *C*$H_2^{2/3}$), 24.3 (s, *C*$H_2^{2/3}$). $^{31}P\{^1H\}$ NMR (DMSO, 121 MHz): -52.0 (broad s, 1P, PTA), -144.21 (h, $^1J_{P-F}$ = 708 Hz, 1P, PF_6). IR ν_{max} (neat)/cm^{-1}: 3360 (NH), 1545 (carbene).

View Article Online
DOI: 10.1039/C7DT03189K

Synthesis of [(1,3,5-triaza-7-phosphaadamantane)Au{C(NHXylyl)(sarcosine)}]PF_6 (12a)

The complex was prepared as described for **11a**, from ClAu{C(NHxylyl)(sarcosine)} (50 mg, 0.104 mmol), 1,3,5-triaza-7-phosphaadamantane (16 mg, 0.104 mmol) and potassium hexafluorophosphate (96 mg, 0.52 mmol). The product was isolated as a pink powder as a mixture of two stereoisomers in a ratio 3/1 (66 mg, 0.09 mmol, 85%). Anal. Calcd for $C_{20}H_{32}N_5O_2PAuPF_6$ (747.41): C, 32.14; H, 4.32; N, 9.37. Found: C, 32.05; H, 4.36; N, 9.42. ^{1}H NMR (CD_3CN, 300 MHz): δ 8.31 (broad s, 0.75H, NH isomer 1), 8.20 (broad s, 0.25H, NH isomer 2), 7.23 (m, 3H, $CH_{arom.}$), 4.55 (s, 1.5H, NCH_2 isomer 1), 4.45 (d, $^3J_{H\text{-}H}$ = 13 Hz, 3H, NCH_2N), 4.34 (d, $^3J_{H\text{-}H}$ = 13 Hz, 3H, NCH_2N), 4.26 (s, 0.5H, NCH_2 isomer 2), 4.23 (q, $^3J_{H\text{-}H}$ = 7 Hz, 2H, OCH_2), 3.96 (s, 6H, PCH_2N), 3.45 (s, 0.7H, NCH_3 isomer 2), 3.13 (s, 2.3H, NCH_3 isomer 1), 2.24 (s, 6H, $CH_{3\ xylyl}$), 1.27 (q, $^3J_{H\text{-}H}$ = 7 Hz, 3H, $CH_2\underline{CH_3}$). $^{13}C\{^1H\}$ NMR (CD_3CN, 75 MHz): only major isomer observed, ($C_{carbene}$ not visible), 169.8 (s, *C*=O), 137.8 (s, $C_{arom.\ ipso}$), 129.6 (s, $C_{arom.\ ortho}$), 129.3 (s, $CH_{arom.}$), 73.1 (d, $^3J_{P\text{-}C}$ = 8 Hz, NCH_2N), 62.6 (s, OCH_2), 60.5 (s, NCH_2 observed by $^1H\text{-}^{13}C\{^1H\}$ correlation), 51.4 (d, $^1J_{P\text{-}C}$ = 19 Hz, PCH_2N), 37.4 (s, NCH_3), 18.7 (s, $CH_{3\ xylyl}$). 14.6 (s, $CH_2\underline{CH_3}$). $^{31}P\{^1H\}$ NMR (CD_3CN, 121 MHz): -52.4 (broad s, 1P, PTA), -144.6 (h, $^1J_{P\text{-}F}$ = 708 Hz, 1P, PF_6). IR ν_{max} (neat)/cm^{-1}: 3340 (NH), 1740 (C=O), 1554 (carbene).

Synthesis of [(1,3,5-triaza-7-phosphaadamantane)Au{C(NH^{t}Bu)(sarcosine)}]PF_6 (12b)

The complex was prepared as described for **11a**, from ClAu{C(NH^{t}Bu)(sarcosine)} (50 mg, 0.12 mmol), 1,3,5-triaza-7-phosphaadamantane (19 mg, 0.12 mmol) and potassium hexafluorophosphate (110 mg, 0.60 mmol) as a red powder which was a mixture of four stereoisomers in a ratio 46/24/21/9. (38 mg, 0.05 mmol, 45%,). Anal. Calcd for $C_{16}H_{32}N_5O_2PAuPF_6$ (699.37): C, 27.48; H, 4.61; N, 10.01. Found: C, 27.53; H, 4.58; N, 9.90. ^{1}H NMR (DMSO, 300 MHz): δ 9.16 (s, 0.21H, NH isomer 3), 8.12 (s, 0.24H, NH isomer 3), 7.66 (s, 0.09H, NH isomer 4), 7.52 (s, 0.46H, NH isomer 1), 4.72 (s, 1H, NCH_2 isomer 1), 4.54 (d, $^3J_{H\text{-}H}$ = 13 Hz, 3H, NCH_2N), 4.45 (s, 0.5H, NCH_2 isomer 2), 3.45 (m, 9.4H, NCH_2N + PCH_2N + NCH_2 isomer 3 and 4), 4.17 (q, $^3J_{H\text{-}H}$ = 7 Hz, 2H, OCH_2), 3.45 (s, 0.6H, NCH_3 isomer 3 and 4), 3.04 (s, 0.7H, NCH_3 isomer 2), 2.97 (s, 1.5H, NCH_3 isomer 1), 1.52 (s, 4.3H, ^{t}Bu isomer 1), 1.49 (s, 2.4H, ^{t}Bu isomer 2), 1.32 (s, 2.9H, ^{t}Bu isomer 3 and 4), 1.24 (t, $^3J_{H\text{-}H}$ = 7 Hz, 3H, $CH_2\underline{CH_3}$). $^{13}C\{^1H\}$ NMR (DMSO, 75 MHz): only major isomer observed, ($C_{carbene}$ not visible), 169. (s, *C*=O), 71.8 (d, $^3J_{P\text{-}C}$ = 8 Hz, NCH_2N), 61.2 (s, OCH_2), 61.1 (s, NCH_2), 54.3 (s, $C(CH_3)_3$), 50.4 (d, $^1J_{P\text{-}C}$ = 19 Hz, PCH_2N), 36.4 (s, NCH_3), 31.7 (s, $C(CH_3)_3$), 14.2 (s,

View Article Online
DOI: 10.1039/C7DT03189K

$CH_2\underline{C}H_3$). $^{31}P\{^1H\}$ NMR (DMSO, 121 MHz): -50.4 (broad s, 1P, PTA), -144.22 (h, $^1J_{P-F}$ = 708 Hz, 1P, PF_6). IR ν_{max} (neat)/cm^{-1}: 3354 (NH), 1740 (C=O), 1549 (carbene).

Synthesis of [(^{Ad}CAAC)Au(CNxylyl)]SbF_6 (13a)

A Schlenk flask was charged with (^{Ad}CAAC)AuCl (121 mg, 0.2 mmol), $AgSbF_6$ (70 mg, 0.2 mmol) and CH_2Cl_2 (2 mL). The resulting suspension was stirred for 1 h in the dark. The mixture was filtered through a Celite pad (2 cm), which was washed with another 8 mL of CH_2Cl_2. The colourless solution was concentrated to *ca.* 2 mL and an excess of xylyl isocyanide (52 mg, 0.4 mmol) was added, followed by stirring at room temperature for 4 h. The solution was concentrated and the product precipitated with hexanes (15 mL), centrifuged and washed with hexanes (5 mL). The volatiles were removed under vacuum to give the complex as a white solid (169 mg, 0.18 mmol, 90 %). Anal. Calcd. for $C_{36}H_{48}AuF_6N_2Sb$ (940.24): C, 45.93; H, 5.14; N, 2.98. Found: C, 45.82; H, 5.04; N, 3.03. ^1H NMR (300 MHz, CD_2Cl_2): δ 7.53 (t, *J* = 8.0 Hz, 1H, CH-aromatic), 7.39–7.34 (m, 2H CH-meta aniline and 1H CH-para CNxylyl), 7.18 (d, *J* = 7.6 Hz, CH-aromatic CNxylyl), 3.48 (br d, *J* = 12.2 Hz, 2H, CH_2), 2.77 (sept, *J* = 6.7 Hz, 2H, C$\underline{H}(CH_3)_2$), 2.45–1.86 (m, 14H, adamantyl CH and CH_2), 2.27 (s, 6H, $2CH_3$, CNxylyl), 1.44 (s, 6H, $2CH_3$), 1.38 (d, *J* = 6.7 Hz, 6H, CH(C$\underline{H}_3)_2$) overlapping with 1.36 (d, *J* = 6.7 Hz, 6H, CH(C$\underline{H}_3)_2$) ppm. $^{13}C\{^1H\}$ NMR (75 MHz, CD_2Cl_2): δ 246.5 (C carbene), 145.3 (*o*-C aniline), 136.9 (*o*-C, CNxylyl) 135.2 (C_{ipso} aniline), 132.2 (*p*-CH, CNxylyl), 131.0 (*p*-CH, aniline), 128.9 (*m*-CH, CNxylyl), 125.8 (*m*-CH aniline), 123.5 (N$\underline{C}_{ipso}$ CNxylyl), 80.1 (C_q), 65.4 (C_q), 48.5 (CH_2), 38.9 (CH_2), 37.4, 36.7, 34.4 (CH_2), 29.5, 29.4, 28.3, 27.2, 27.1, 23.2, 18.6 ($\underline{C}H_3$ CNxylyl) ppm. IR ν_{max} (neat)/cm^{-1}: 2215 (CNxylyl).

Synthesis of [(^{Ad}CAAC)Au{C(NHxylyl)(pyrrolidine)}]SbF_6 (14a)

The solution of **13a** (50 mg, 0.053 mmol) and pyrrolidine (9 µL, 0.106 mmol) in 6 mL of MeCN was stirred overnight in the dark, filtered through a thin layer of Celite, washed with a saturated ammonium chloride solution, and dried with sodium sulphate. The solution was filtered and volatiles were removed under vacuum. The residue was taken up in dichloromethane and the product was precipitated with hexane as a white powder (41 mg, 0.040 mmol, 75%). Anal. Calcd. for $C_{40}H_{57}AuF_6N_3Sb$ (1011.32): C, 47.44; H, 5.67; N, 4.15. Found: C, 47.55; H, 5.78; N, 4.36. ^1H NMR (300 MHz, CD_2Cl_2): δ 7.46 (t, *J* = 8.2 Hz, 1H, *p*-CH aniline), 7.32 (t, 2H *m*-CH aniline), 7.18 (t, *J* = 6.1 Hz, 1H, *p*-CH xylyl), 7.10 (d, *J* = 6.1 Hz, *m*-CH xylyl), 6.85 (br s, 1H, NH), 3.28 (t, *J* = 7.1 Hz, 2H, NCH_2 (C4) pyrrolidine), 2.71

View Article Online
DOI: 10.1039/C7DT03189K

(sept, J = 6.7 Hz, 2H, C<u>*H*</u>$(CH_3)_2$), 2.59 (br d, J = 10.2 Hz, 2H, CH_2), 2.48 (t, J = 6.7 Hz, 2H, NCH_2 (C1) pyrrolidine), 2.25–1.53 (m, 14H, adamantyl CH and CH_2) overlapping with 2.12 (s, 6H, $2CH_3$, CNxylyl) and 2.00 (m, J = 7.1 Hz, 2H, CH_2 (C3) pyrrolidine) and 1.58 (m, 2H, CH_2 (C2) pyrrolidine), 1.32 (s, 6H, $2CH_3$) overlapping with 1.33 (d, J = 6.7 Hz, 6H, CH(C<u>*H*</u>$_3)_2$) and 1.31 (d, J = 6.7 Hz, 6H, CH(C<u>*H*</u>$_3)_2$) ppm. $^{13}C\{^1H\}$ NMR (75 MHz, CD_2Cl_2): δ 255.6 (C carbene CAAC), 201.6 (C open chain carbene), 145.6 (*o*-C aniline), 137.5 (N<u>C</u>$_{ipso}$ CNxylyl), 136.9 (*o*-C, CNxylyl), 136.4 (C_{ipso} aniline), 130.3 (*p*-CH, aniline), 129.1 (*p*-CH overlapping with *m*-CH, CNxylyl), 125.7 (*m*-CH aniline), 79.0 (C_q), 65.5 (C_q), 53.86 (NCH_2, C1 pyrrolidine overlaps with residual $CHDCl_2$), 48.7 (CH_2), 46.0 (NCH_2 C4 pyrrolidine), 38.8 (CH_2), 37.3, 35.2, 34.3 (CH_2), 29.5, 29.4, 28.0, 27.2, 26.5, 25.1 (CH2, C3 pyrrolidine), 24.7 (CH2, C2 pyrrolidine), 23.2 (CH_3), 18.7 (<u>*C*</u>H_3 CNxylyl) ppm. IR ν_{max} (neat)/cm^{-1}: 3331 (NH), 1546 (carbene).

Biological testing

Antiproliferation assay. Human HL 60 and A549 cancer cell lines (from ECACC) were cultured in RPMI 1640 medium with 10% fetal calf serum, 2mM L-glutamine, 100U/mL penicillin and 100 µg/mL streptomycin (Invitrogen). Cells were maintained in a humidified atmosphere at 37 °C and 5% CO_2. The human MCF-7 cancer cell line (from ECACC) were cultured in DMEM medium with 10% fetal calf serum, 2mM L-glutamine, 100U/mL penicillin and 100 µg/mL streptomycin (Invitrogen). Cells were maintained in a humidified atmosphere at 37 °C and 5% CO_2. Inhibition of cancer cell proliferation was measured by the 3-(4,5-dimethylthiazol-2-yl)-5-(3-carboxymethoxyphenyl)-2-(4-sulfophenyl)2H-tetrazolium (MTS) assay using the CellTiter 96 Aqueous One Solution Cell Proliferation Assay (Promega) and following the manufacturer's instructions. Briefly, cells (3×10^4/100 µL for HL 60 and 8×10^3/100 µL for both A549 and MCF-7) were seeded in 96-well plates and left untreated or treated with 1 µL of DMSO (vehicle control) or 1 µL of complexes diluted in DMSO at different concentrations in triplicate for 72 h at 37 °C with 5% CO_2. Following this, MTS assay reagent was added for 4 h and absorbance measured at 490 nm using a Polarstar Optima microplate reader (BMG Labtech). IC_{50} values were calculated using GraphPad Prism Version 5.0 software.

Inhibition of mammalian Thioredoxin Reductase

To determine the inhibition of mammalian TrxR, an established microplate-reader-based assay was performed. (**Ref**: Chem. Eur. J. 2017, 23, 1869 – 1880) For this purpose,

View Article Online
DOI: 10.1039/C7DT03189K

commercially available rat liver TrxR (Sigma Aldrich) was used and diluted with distilled water to achieve a concentration of 3.58 U/mL. The compounds were freshly dissolved as stock solutions in DMSO. Aliquots (25 mL) of the enzyme solution and either potassium phosphate buffer (25 µL; pH 7.0) containing the compounds in graded concentrations or buffer (25 µL) without the compounds, but DMSO (positive control) were added. A blank solution (DMSO in buffer; 50µL) was also prepared (final concentrations of DMSO: 0.5% v/v). The resulting solutions were incubated with moderate shaking for 75 min at 37°C in a 96-well plate. A portion (225 µL) of reaction mixture (1 mL of reaction mixture consists of: 500 µL potassium phosphate buffer pH 7.0, 80 µL EDTA solution (100 mM, pH 7.5), 20 µL BSA solution (0.2 %), 100 µL of NADPH solution (20 mM), and 300 µL distilled water) was added to each well and the reaction was immediately initiated by the addition of 20 mM ethanolic DTNB solution (25 µL). After thorough mixing, the formation of 5-TNB was monitored with a microplate reader at 405 nm ten times in 35 second intervals for about 6 min. The increase in 5-TNB concentration over time followed a linear trend ($r^2 = 0.990$), and the enzymatic activities were calculated as the slopes (increase in absorbance per second) thereof. For each tested compound, the non-interference with the assay components was confirmed by a negative control experiment using an enzyme-free test solution. IC_{50} values were calculated as the concentration of the compound decreasing the enzymatic activity of the untreated control by 50%, and are given as the means and error of three repeated experiments.

ROS assay. 100 µL of A549 cells were seeded at a density of 1 x 10^5 cells/mL in a 96-well black plate with a transparent bottom. The cells were incubated at 37 °C for 24h. The medium was removed, and replaced with 50 µM H_2DCFDA in phosphate buffer solution for 40 min. H_2DCFDA was removed and replaced with fresh medium and the cells were left for recovery for 20 min at 37 °C. Basal fluorescence was measured at 485/520 nm on a POLARstar Optima. Cells were incubated with 10 µM, 50µM, or 100 µM of compounds, 1% DMSO (negative control) and 100 µM of H_2O_2 (positive control) for 24h. Fluorescence was read at 485/520 nm. Basal fluorescence was subtracted from the fluorescence in treated cells to calculate the amount of fluorescence caused by the compounds.

X-Ray Crystallography.

View Article Online
DOI: 10.1039/C7DT03189K

Crystals suitable for X-ray diffraction were obtained by the slow evaporation of dichloromethane/hexane solutions for **9a**, **10a**, **10b** and **14a**, acetone/toluene solutions for **11a** and **11b**, or by layering a CH_2Cl_2 solution with hexanes for **13a**. Complex **11a** crystallizes as a solvate with one disordered molecule of CH_2Cl_2. Two positions for CH_2Cl_2 molecule were successfully resolved upon cooling the crystal of **11a** to 140 K leading to occupancies 0.6 and 0.4. The disordered CH_2Cl_2 molecule was refined in the geometry of isosceles triangle and DFIX restraints on C1S–Cl1 bond length (1.72(1) Å) and Cl1···Cl2 distance (2.90(1) Å). The atom C3 was disordered over two half-populated positions for complex **14a**. Crystals were mounted in oil on glass fibres and fixed in the cold nitrogen stream on a diffractometer. Data were collected using an Oxford Diffraction Xcalibur-3/Sapphire3-CCD diffractometer, using graphite monochromated Mo K_α radiation (λ = 0.71073 Å) at 140 K. Data were processed using CrystAlisPro-CCD and –RED software.[40] The principal crystallographic data and refinement parameters are listed in Table 4. The structures were solved by direct methods and refined by the full-matrix least-squares against F^2 in an anisotropic (for non-hydrogen atoms) approximation. All hydrogen atom positions were refined in isotropic approximation in "riding" model with the $U_{iso}(H)$ parameters equal to 1.2 $U_{eq}(C_i)$, for methyl groups equal to 1.5 $U_{eq}(C_{ii})$, where $U(C_i)$ and $U(C_{ii})$ are respectively the equivalent thermal parameters of the carbon atoms to which the corresponding H atoms are bonded. All calculations were performed using the SHELXTL software.[41]

Table 4. Summary of crystallographic data and structure refinement

	9a	**10a**	**10b**	**11a**	**13a**	**14a**
CCDC number	1568251	1568247	1568252	1568248	1568249	1568250
Temperature (K)	140	100	100	140.0	140	100
Empirical formula	$C_{13}H_{18}AuClN_2$	$C_{14}H_{20}AuClN_2O_2$	$C_{10}H_{20}AuClN_2O_2$	$C_{20}H_{32}AuCl_2F_6N_5P_2$	$C_{36}H_{48}AuF_6N_2Sb$	$C_{40}H_{57}AuF_6N_3Sb$
Molecular weight	434.71	480.74	432.70	786.31	941.48	1012.60
Crystal system	Monoclinic	Orthorhombic	Monoclinic	Monoclinic	Monoclinic	Monoclinic
Space group	$P2_1/c$	$P2_12_12_1$	$P2_1/c$	$P2_1/n$	$P2_1/c$	$P2_1/n$
Crystal colour, habit	Colourless/block	Colourless/needle	Colourless/block	Colourless/block	Colourless/plate	Colourless/block
Crystal size (mm)	0.23×0.15×0.08	0.20×0.05×0.05	0.08×0.04×0.04	0.18×0.07×0.06	0.27×0.16×0.09	0.08×0.07×0.05
a (Å)	7.3404(2)	10.5095(2)	12.0876(2)	13.6153(2)	9.9471(3)	9.7273(3)
b (Å)	13.3484(3)	12.0198(3)	9.43950(10)	12.5760(2)	26.0651(8)	13.1815(3)
c (Å)	14.7732(4)	13.0933(2)	13.5065(2)	16.6816(3)	13.5998(5)	30.9171(11)
α (°)	90	90	90	90	90	90
β (°)	102.267(2)	90	114.107(2)	106.059(2)	95.681(3)	91.749(4)
γ (°)	90	90	90	90	90	90
V (Å^3)	1414.47(6)	1653.97(6)	1406.69(3)	2744.86(8)	3508.7(2)	3962.4(2)
Z	4	4	4	4	4	4
D_{calc} (g cm^{-3})	2.041	1.931	2.043	1.903	1.782	1.697
$2\theta_{max}$ (°)	28.00	27.48	27.48	28.00	26.37	27.49

Abs. coeff., μ(Mo-K_α) (cm^{-1})	10.570	9.058	10.638	5.732	5.006	4.440
T_{max}/T_{min}	0.4852/0.1948	0.6601/0.2645	0.6756/0.4832	0.7249/0.4252	0.6615/0.3451	0.8085/0.7177
collected reflections	13835	27496	16303	28505	24982	27773
independent reflections	3419	3780	3218	6603	7155	9081
observed reflections ($I > 2\sigma(I)$)	3273	3659	3132	6075	6372	8662
R_{int}	0.0270	0.0654	0.0254	0.0270	0.0364	0.0282
Number of parameters	170	185	150	355	423	471
R_1 (on F for observed	0.0205	0.0256	0.0125	0.0234	0.0211	0.0269
wR_2 (on F^2 for all reflexions)	0.0544	0.0557	0.0278	0.0596	0.0441	0.0638
Weighting scheme	$w^{-1}=\sigma^2(F_o^2) + (aP)^2 + bP$, where $P = 1/3(F_o^2 + 2F_c^2)$					
A	0.03	0.03	0.01	0.03	0.008	0.03
B	1.8	0.1	2.1	2.5	2.3	5.7
F(000)	824	920	824	1536	1848	2008
Goodness-of-fit	1.051	1.027	0.892	1.041	1.047	1.041
$\Delta\rho_{max}/\Delta\rho_{max}$ (e $Å^{-3}$)	0.903/–1.138	1.484/–1.226	0.424/–0.345	0.927/–0.829	0.420/–0.556	1.198/–1.195

View Article Online
DOI: 10.1039/C7DT03189K

References

1 I. Ott, *Coord. Chem. Rev.,* 2009, **253**, 1670.

2 A. Gautier and F. Cisnetti, *Metallomics,* 2012, **4**, 23.

3 R. Rubbiani, E. Schuh, A. Meyer, J. Lemke, J. Wimberg, N. Metzler-Nolte, F. Meyer, F. Mohr and I. Ott, *Med. Chem. Commun*., 2013, **4**, 942.

4 A. Citta, Esther Schuh, F. Mohr, A. Folda, M. L. Massimino, A. Bindoli, A. Casini and M. P. Rigobello, *Metallomics,* 2013, **5**, 1006.

5 B. Bertrand and A. Casini, *Dalton Trans*., 2014, **43**, 4209.

6 (a) W. Liu and R. Gust, *Chem. Soc. Rev.,* 2013, **42**, 755. (b) W. Liu and R. Gust, *Coord. Chem. Rev*., 2016, **329**, 191.

7 C. Duncan and A. R. White, *Metallomics*, 2012, **4**, 127.

8 L. Ruiz-Azuara and M.E. Bravo-Gómez, *Curr. Med. Chem.,* 2010, **17***,* 3606.

9 B. M. Paterson and P. S. Donnelly, *Chem. Soc. Rev*., 2011, **40**, 3005.

10 M.-L. Teyssot, A.-S. Jarrousse, A. Chevry, A. De Haze, C. Beaudoin, M. Manin, S. P. Nolan, S. Díez-González, L. Morel and A. Gautier, *Chem. Eur. J.,* 2009, **15**, 314.

11 W. Streciwilk, F. Hackenberg, H. Müller-Bunz and M. Tacke, *Polyhedron,* 2014, **80**, 3.

12 M. Tacke, *J. Organomet. Chem.,* 2015, **782**, 17.

13 L. Eloy, A.-S. Jarrousse, M.-L. Teyssot, A. Gautier, L. Morel, C. Jolivalt, T. Cresteil and S. Roland, *ChemMedChem,* 2012, **7**, 805.

14 M. Marinelli, M. Pellei, C. Cimarelli, H. V. R. Dias, C. Marzano, F. Tisato, M. Porchia, V. Gandin and C. Santini, *J. Organomet. Chem.,* 2016, **806**, 45.

15 M. Asif, M. Ad. Iqbal, M. A. Hussein, C. E. Oon, R. A. Haque, M. B. Khadeer Ahamed, A. S. A. Majid and A. M. S. A. Majid, *Eur. J. Med. Chem*., 2016, **108**, 177.

16 M. Z. Ghdhayeb, R. A. Haque, S. Budagumpi, M. B. Khadeer Ahamed and A. M. S. A. Majid, *Polyhedron,* 2017, **121**, 222.

17 H. M. J. Wang and I. J. B. Lin, *Organometallics,* 1998, **17**, 972.

18 J. P. Canal, T. Ramnial and J. A. C. Clyburne, A carbene transfer agent, in: Roesky, H. W.; Kennepohl, D. K (eds), Experiments in Green and Sustainable Chemistry, Wiley-VCH, Weinheim, 2009, p. 25ff.

19 (a) V. Lavallo, Y. Canac,C. Prasang, B. Donnadieu and G. Bertrand, *Angew. Chem. Int. Ed*., 2005, **44**, 5705; (b) V. Lavallo, Y. Canac, A. DeHope, B. Donnadieu and G. Bertrand, *Angew. Chem. Int. Ed*., 2005, **44**, 7236. (c) G. D. Frey, R. D. Dewhurst, S. Kousar, B. Donnadieu and G. Bertrand, *J. Organomet. Chem*., 2008, **693**, 1674. (d) V.

View Article Online
DOI: 10.1039/C7DT03189K

Lavallo, G. D. Frey, S. Kousar, B. Donnadieu and G. Bertrand, *Proc. Nat. Acad. Sci. USA*, 2007, **104**, 13569.

20 M, Soleilhavoup and G. Bertrand, *Acc. Chem. Res*., 2015, **48**, 256.

21 A. S. Romanov and M. Bochmann, *Organometallics,* 2015, **34**, 2439.

22 For photochemical applications of CAAC complexes see (a) A. S. Romanov, D. Di, Le Yang, J. Fernandez-Cestau, C. R. Becker, C. E. James, B. Zhu, M. Linnolahti, D. Credgington and M. Bochmann, *Chem. Commun.,* 2016, **52**, 6379; (b) A. S. Romanov, C. R. Becker, C. E. James, D. Di, D. Credgington, M. Linnolahti and M. Bochmann, *Chem. Eur. J.,* 2017, **23**, 4625; (c) M. Gernert, U. Müller, M. Haehnel, J. Pflaum and A. Steffen, *Chem. Eur. J.,* 2017, **23**, 2206; (d) D. Di, A. S. Romanov, L. Yang, J. M. Richter, J. P. H. Rivett, S. Jones, T. H. Thomas, M. Abdi Jalebi, R. H. Friend, M. Linnolahti, M. Bochmann and D. Credgington, *Science,* 2017, **356**, 159.

23 (a) D. S. Weinberger, M. Melaimi, C. E. Moore, A. L. Rheingold, G. Frenking, P. Jerabek and G. Bertrand, *Angew. Chem. Int. Ed*., 2013, **52**, 8964; b) D. S. Weinberger, N. Amin SK, K. C. Mondal, M. Melaimi, G. Bertrand, A. C. Stückl, H. W. Roesky, B. Dittrich, S. Demeshko, B. Schwederski, W. Kaim, P. Jerabek, and G. Frenking, *J. Am. Chem. Soc*., 2014, **136**, 6235.

24 A. S. Romanov and M. Bochmann, *J. Organomet. Chem*., 2017, in press. DOI: 10.1016/j.jorganchem.2017.02.045.

25 F. Kolundžić, A. Murali, P. Prez-Galn, J. O. Bauer, C. Strohmann, K. Kumar, and H. Waldmann, *Angew. Chem. Int. Ed.,* 2014, **53**, 8122.

26 (a) F. Bonati and G. Minghetti, *J. Organomet. Chem.,* 1973, **59**, 403; (b) G. Minghetti and F. Bonati, *Inorg. Chem*., 1974, **13**, 1600; (c) J. E. Parks and A. L. Balch, *J. Organomet. Chem*., 1974, **71**, 453. (d) M. Williams, A. I. Green, J. Fernandez-Cestau, D. L. Hughes, M. A. O'Connell, M. Searcey, B. Bertrand and M. Bochmann, *Dalton Trans.,* 2017, **46**, 13397.

27 (a) S. Montanel-Pérez, R. P. Herrera, A. Laguna, M. D. Villacampa and M. C. Gimeno, *Dalton Trans*., 2015, **44**, 9052. (b) For studies on amino ester decorated NHC complexes see also: F. Schmitt, K. Donnelly, J. K. Muenzner, T. Rehm, V. Novohradsky, V. Brabec, J. Kasparkova, M. Albrecht, R. Schobert and T. Mueller, *J. Inorg. Biochem*. 2016, **163**, 221.

28 A. S. K. Hashmi, T. Hengst, C. Lothschutz and F. Rominger, *Adv. Synth. Catal.* 2010, **352**, 1315.

29 B. J. Coe and S. J. Glenwright, *Coord. Chem. Rev.,* 2000, **203**, 5.

View Article Online
DOI: 10.1039/C7DT03189K

30 A. Bindoli, M. P. Rigobello, G. Scutari, C. Gabbiani, A. Casini and L. Messori, *Coord. Chem. Rev.,* 2009, **253**, 1692.

31 A. Casini, C. Gabbiani, F. Sorrentino, M. P. Rigobello, A. Bindoli, T J. Geldbach, A. Marrone, N. Re, C. G. Hartinger, P. J. Dyson and L. Messori, *J. Med. Chem.,* 2008, **51**, 6773.

32 A. Citta, A. Folda, A. Bindoli, P. Pigeon, S. Top, A. Vessieres, M Salmain, G. Jaouen and M. P. Rigobello, *J. Med. Chem.,* 2014, **57**, 8849.

33 M. P. Rigobello, L. Messori, G. Marcon, M. A. Cinellu, M. Bragadin, A. Folda, G. Scrutari and A. Bindoli, *J. Inorg. Biochem.,* 2004, **98***,* 1634.

34 (a) J. L. Hickey, R. A. Ruhayel, P. J. Barnard, M. V. Baker, S. J. Berners-Price and A. Filipovska, *J. Am. Chem. Soc.,* 2008, **130**, 12570; (b) B. Bertrand, A. de Almeida, E. P. M. van der Burgt, M. Picquet, A. Citta, A. Folda, M. P. Rigobello, P. Le Gendre, E. Bodio and A. Casini, *Eur. J. Inorg. Chem.,* 2014**, 27**, 4532.

35 R. Rubbiani, I. Kitanovic, H. Alborzinia, S. Can, A. Kitanovic, L. A. Onambele, M. Stefanopoulou, Y. Geldmacher, W. S. Sheldrick, G. Wolber, A. Prokop, S. Wolfl and I. Ott, *J. Med. Chem*., 2010, **53**, 8608.

36 (a) R. Rubbiani, S. Can, I. Kitanovic, H. Alborzinia, M. Stefanopoulou, M. Kokoschka, S. Mönchgesang, W. S. Sheldrick, S. Wölfl and I. Ott, *J. Med. Chem.,* 2011, **54**, 8646; (b) C. Schmidt, B. Karge, R. Misgeld, A. Prokop, M. Brönstrup and I. Ott, *Med. Chem. Commun.,* 2017, DOI: 10.1039/C7MD00269F.

37 J. K. Muenzner, B. Biersack A. Albrecht, T. Rehm, U. Lacher, W. Milius, A. Casini J.-J. Zhang, I. Ott V. Brabec, O. Stuchlikova, I. C. Andronache, L. Kaps D. Schuppan and R. Schobert, *Chem. Eur. J.,* 2016, **22**, 18953.

38 U. Jungwirth, C. R. Kowol, B K. Keppler, C. G. Hartinger, W. Berger and P. Heffeter, *Antioxid. Redox. Signal.,* 2011, **15**, 1085.

39 G. Gritzner and J. Kůta, *Electrochim. Acta,* 1984, **29**, 869.

40 *Programs CrysAlisPro*, Oxford Diffraction Ltd., Abingdon, UK (2010).

41 G.M. Sheldrick, *Acta Cryst.,* 2008, **A64**, 112.

View Article Online
DOI: 10.1039/C7DT03189K

Table of Content

Synthesis of group 11 metals CAAC and acyclic carbene complexes with low micromolar cytotoxicity on human cancer cells.